A Measurement Method Based on RF Deflector for Particle Bunch Longitudinal Parameters in Linear Accelerators

Luca Sabato, Pasquale Arpaia, *Senior Member, IEEE*, Antonio Gilardi, *Graduate Student Member, IEEE*, Andrea Mostacci, Luigi Palumbo, and Alessandro Variola

***Abstract*— In high-brightness electron linear accelerators (LINACs), the particle bunch length is measured by a radio frequency deflector (RFD). The electron bunch is deflected vertically toward a screen and its length can be obtained using vertical spot size measurements after a proper calibration, e.g., measuring the vertical bunch centroid while varying the deflecting voltage phase. The energy parameters of the bunch (the energy chirp and the energy spread) and the correlation between particle positions, divergences, and energies contribute to the bunch vertical dimension at the screen position after the RFD and so far were considered as a source of systematic errors in a bunch length measurement. The measurement theory and production model for bunch length, energy spread and chirp, as well as correlations are described. As usual in particle accelerators physics, the method is validated using numerical simulations of state-of-the-art LINACs with a reference simulation code showing a typical accuracy in the few percent levels.**

***Index Terms*— Electron accelerators, high energy physics instrumentation computing, instruments, linear particle accelerator, particle beam measurements.**

I. Introduction

IN HIGH-BRIGHTNESS electron linear accelerators (LINACs), the bunch length is measured very often by means of an indirect and disruptive method based on a radio frequency deflector (RFD) [1]. RFD provides a transverse kick to the electron bunch, introducing a relationship between the bunch length and the transverse footprint (spot size) at a screen placed after the RFD [2]. Spot size measurements are quite common (and easily doable) in LINACs, but one of the reasons of the enormous spread of this technique is the possibility of a self-calibration by measuring the deviation of the bunch centroid induced by varying the beam arrival time at the RFD (i.e., the deflecting voltage phase) [3]. This method allows to measure the length of ultrashort electron beams down to a few femtoseconds [4], and the combination of an RFD with a dispersive element (e.g., dipole magnet) allows the measurement of the longitudinal beam phase space [5].

Most of the high brightness of LINACs that are nowadays undergoing a worldwide research and development effort can be roughly divided into three classes. The first kind concerns gamma ray source based on the Compton effect, where a high-brightness electron beam collides with high intensity photon beam [6]. The short (ps-scale) electron bunches must have a tight pointing stability as well as small energy spread and chirp. Transverse wakefields, responsible of jitters in the beam transverse position at the collision point, directly affect the correlations between particle positions and divergences. The second class concerns modern free electron laser (FEL) injector where the beam is hundreds of femtosecond long (to achieve tens of kiloampere peak currents) and the energy spread must be extremely small, at the few ‰ level. Another kind of high-brightness LINACs are plasma based accelerators [7] where the extremely high accelerating field could allow orders of magnitude reduction in accelerator dimensions. In the actual prototypes of those machines, ultrashort (tens of femtoseconds) bunches are affected by huge energy spread and chirps, nowadays limiting their performances, and they need to be carefully measured. Since RFDs are very common in high-brightness LINACs [8]–[10] due to their very high resolutions, as state-of-the-art methods [11], however, an extended metrological theory behind this measurement method, capable of highlighting all the terms affecting the bunch length measurement, is still missing. The standard technique is based on the assumptions of negligible energy spread and/or correlation between particle longitudinal positions and energies (namely, energy chirp) and/or correlations between particle positions, divergence, and energies at the RFD location. These parameters affect the vertical spot size at the measurement screen [12].

In this article, it is proposed an original RFD-based measurement method of the energy chirp and spread, as well as of the correlations among vertical and longitudinal positions, vertical positions and energies, vertical divergences and longitudinal positions, and vertical divergences and energies of the particles within the electron bunch. The main advantage

Manuscript received February 29, 2020; accepted June 22, 2020. Date of publication July 15, 2020; date of current version December 7, 2020. The Associate Editor coordinating the review process was Shoaib Amin. *(Corresponding author: Pasquale Arpaia.)*

Luca Sabato is with CERN, 01211 Geneva, Switzerland.

Pasquale Arpaia and Antonio Gilardi are with CERN, 01211 Geneva, Switzerland, and also with IMPALab, Department of Electrical Engineering and Information Technology, University of Naples Federico II, 80138 Naples, Italy (e-mail: pasquale.arpaia@unina.it).

Andrea Mostacci and Luigi Palumbo are with the Department of Basic and Applied Sciences for Engineering, Sapienza University of Rome, 00161 Rome, Italy.

Alessandro Variola is with INFN, 00044 Frascati, Italy.

Digital Object Identifier 10.1109/TIM.2020.3009342

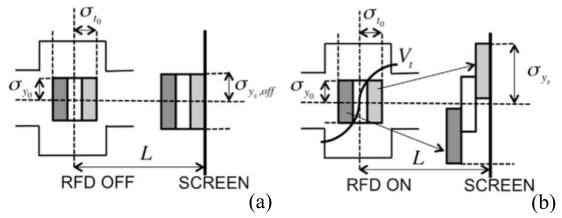

Fig. 1. Overview of the measurement technique with (a) RFD OFF and (b) RFD ON for a bunch traveling from left to right: σ_{y0} is the vertical dimension of the bunch at the RFD center, L is the distance between the RFD center and the screen, V_t is the deflecting voltage amplitude, σ_{t0} is the bunch length, and $\sigma_{y_s,\mathrm{OFF}}$ and σ_{y_s} are the vertical spot sizes at the screen when the RFD is OFF and ON, respectively [22].

of the results is to measure the energy spread, energy chirp, and the bunch length using only the RFD without the need of a subsequent dispersive section. Such idea can have a highly beneficial effect in the design of novel, compact, high gradient accelerators where the diagnostics for measuring single bunch and bunch train should also be squeezed [13]–[15], maintaining the high performance to achieve suitable brightness beams [16], [17]. The case studies cover parameter range relevant for the state-of-the-art LINACs discussed earlier. The Compton source case study is the gamma beam source (GBS) being built in the context of extreme light infrastructure to study nuclear physics (ELI-NP) [18]. The GBS at ELI-NP is meant to be an advanced source of up to 20-MeV gamma rays (tunable between 1 and 20 MeV) to cover a broad range of science: frontier fundamental physics, new nuclear physics and astrophysics as well as applications in nuclear materials, radioactive waste management, material science, and life sciences [19]. For the other two classes, namely FELs and plasma accelerators, the parameters chosen for the four case studies (two cases for each kind of machine) are typical in most of the designs [20].

In Section II, the theory behind this measurement technique is treated and the vertical spot size at the screen placed after the RFD is assessed analytically, without assumptions on the bunch parameters at the RFD entrance. In Section III, the proposed measurement technique is stated formally, by defining the underlying theory and the measurement production model for each measurand. In Section IV, results are validated according to standards used in accelerator engineering, i.e., with reference tracking codes certified against measurements in several operating LINACs; the electron generation and tracking (ELEGANT) code [21] is used.

II. Theoretical Analysis

Fig. 1 shows an overview of the measurement technique; the beam with a spot size σ_{y0} and length σ_{t0} is sent through the RFD. When the RFD is switched OFF (RFD-OFF), the three slices remain centered on the beam axis, and the beam size at the measurement screen $\sigma_{y_s,\mathrm{OFF}}$ depends on the beam divergence and on the length L [see Fig. 1(a)]. When the deflecting voltage is applied (RFD-ON), the colored slices receive a vertical kick (because of the deflecting field) with opposite sign, whereas the white one travels unperturbed since it is at the field zero crossing. Therefore, the spot size at the screen σ_{y_s} depends not only on the beam divergence at the entrance of the RFD but also on the bunch length σ_{t0} as well as on the deflecting voltage [see Fig. 1(b)] [22].

A vertically deflecting RFD is assumed in this article; it is the most common situation since it is practically always used in combination with a horizontal dipole magnet to allow conventional longitudinal phase space measurements.

In this section, the model of the RFD is presented and the particle vertical divergence change due to the RFD is evaluated [see Section (II-A)]. Then, in Sections II-B and II-C, the vertical bunch centroid and spot size at the screen are assessed, respectively.

A. Particle Vertical Divergence Change and RFD Coefficient

An RFD of length L_{RFD} is modeled as an $L_{\mathrm{RFD}}/2$-long drift space, a point-like vertical kick, and another $L_{\mathrm{RFD}}/2$-long drift space [4]. The model neglects the energy chirp and energy spread induced to the bunch by the RFD. Actually, the transverse magnetic TM-like deflecting mode of the cavity has a nonzero derivative of the longitudinal electric field on axis [23]. The vertical kick produces a sudden variation in the particle vertical divergence $\Delta y_0'$ (the bunch parameters at the RFD center are indicated with the subscript 0). Therefore, a particle, while going through the active RFD, experiences a vertical deflecting voltage due to the electric field of the cavity, changing the particle directions. The vertical divergence change depends on the deflecting voltage

$$V(z_0) = V_t \sin(kz_0 + \varphi), \tag{1}$$

where z_0 is the position of the particle along the beam axis assuming the origin in the RFD center, $k = 2\pi f_{\mathrm{RF}}/c$ is the angular wavenumber, f_{RF}, V_t, and φ are the deflecting voltage frequency, amplitude, and phase, respectively, and c is the speed of light. The bunch length is usually much smaller than the RF wavelength (i.e., $kz_0 \ll 1$) and, therefore, the variation of the particle vertical divergence can be written as

$$\Delta y_0'(z_0) = \frac{q}{p_0 c} V(z_0) \approx C_{\mathrm{RFD0}}[kz_0 \cos(\varphi) + \sin(\varphi)] \tag{2}$$

where $C_{\mathrm{RFD0}} = qV_t/(p_0 c)$ is the RFD coefficient, q is the electron charge, and p_0 is the particle momentum at the RFD center [24]. In the ultrarelativistic regime, the RFD coefficient is

$$C_{\mathrm{RFD0}} \approx qV_t/E_0 \tag{3}$$

where E_0 is the particle energy at the RFD center. In this article, $\langle \ldots \rangle$ stands for averaging a quantity over all the particles in the bunch. C_{RFD0} can be approximated at the first order around the bunch average energy $\langle E_0 \rangle$, thus

$$C_{\mathrm{RFD0}} \approx \frac{qV_t}{\langle E_0 \rangle}(1 - \delta_0) = C_{\mathrm{RFD0a}}(1 - \delta_0) \tag{4}$$

where $\delta = (E - \langle E \rangle)/\langle E \rangle$ and $C_{\mathrm{RFD0a}} = qV_t/\langle E_0 \rangle$. The average of C_{RFD0} can be calculated using (4)

$$\langle C_{\mathrm{RFD0}} \rangle \approx \left\langle \frac{V_t}{\langle E_0 \rangle}(1 - \delta_0) \right\rangle = \frac{V_t}{\langle E_0 \rangle} = C_{\mathrm{RFD0a}}. \tag{5}$$

B. Vertical Bunch Centroid

A particle traveling through the RFD is subject to the deflecting voltage, modeled as a vertical kicker at the RFD center [see (2)]. For this reason, the particle vertical divergence becomes $y_0' + \Delta y_0'$ and the equations of the particle vertical motion from the RFD center to the screen are

$$\begin{cases} y_s = y_0 + L\left(y_0' + \Delta y_0'\right) \\ y_s' = y_0' + \Delta y_0' \end{cases} \tag{6}$$

where L is the distance between the RFD center and the screen, and y_s and y_s' are the particle vertical position and divergence at the screen, respectively, with the RFD active.

The vertical bunch centroid at the screen, $C_{y_s} = \langle y_s \rangle$, can be assessed from (2), (5), and (6), assuming the incoming electron bunch travels on axis ($C_{y_0} = \langle y_0 \rangle = 0$ m) and parallel to the accelerator axis ($C_{y_0'} = \langle y_0' \rangle = 0$ rad) itself

$$C_{y_s}(\varphi) = LC_{\mathrm{RFD0a}} \sin(\varphi) - LC_{\mathrm{RFD0a}} 2\pi f_{\mathrm{RF}} \sigma_{t_0\delta_0} \cos(\varphi) \tag{7}$$

where $\sigma_{t_0\delta_0}$ is the energy chirp. For $\varphi \approx 0$ and $\varphi \approx \pi$, the vertical bunch centroid varies linearly with the deflecting voltage phase and the energy chirp gives a constant contribution [22], [25], that is

$$\begin{aligned} C_{y_s}(\varphi \approx 0) &\approx LC_{\mathrm{RFD0a}}\varphi - LC_{\mathrm{RFD0a}} 2\pi f_{\mathrm{RF}} \sigma_{t_0\delta_0} \\ C_{y_s}(\varphi \approx \pi) &\approx LC_{\mathrm{RFD0a}}(\pi - \varphi) + LC_{\mathrm{RFD0a}} 2\pi f_{\mathrm{RF}} \sigma_{t_0\delta_0}. \end{aligned} \tag{8}$$

C. Vertical Spot Size

Keeping only the first-order approximation and considering high-energy electron bunches with low energy spread, the vertical spot size at the screen can be assessed as [25]

$$\begin{aligned} \sigma_{y_s}^2(\varphi) = \sigma_{y_s,\mathrm{OFF}}^2 &+ K_{\mathrm{cal}}^2(\varphi)\sigma_{t_0}^2 - \frac{K_{\mathrm{cal}}^2(\varphi)}{\pi f_{\mathrm{RF}}} \tan(\varphi)\sigma_{t_0\delta_0} \\ &+ \frac{K_{\mathrm{cal}}^2(\varphi)}{(2\pi f_{\mathrm{RF}})^2} \tan^2(\varphi)\sigma_{\delta_0}^2 + 2K_{\mathrm{cal}}(\varphi)\left(\sigma_{y_0t_0} + L\sigma_{y_0't_0}\right) + \\ &- 2\frac{K_{\mathrm{cal}}(\varphi)}{2\pi f_{\mathrm{RF}}} \tan(\varphi)\left(\sigma_{y_0\delta_0} + L\sigma_{y_0'\delta_0}\right), \end{aligned} \tag{9}$$

where $\sigma_{y_s,\mathrm{OFF}}$ is the vertical spot size at the screen with the RFD switched OFF [26], σ_{t_0} the bunch length expressed in seconds, $\sigma_{y_0t_0}$ and $\sigma_{y_0't_0}$ are the covariances between particle vertical positions and longitudinal positions and between particle vertical divergences and longitudinal positions, respectively, $\sigma_{y_0\delta_0}$ and $\sigma_{y_0'\delta_0}$ are the covariances between particle vertical positions and energies and between particle vertical divergences and energies (the elements (3, 6) and (4, 6) of the bunch matrix [27]), respectively, and $K_{\mathrm{cal}}(\varphi)$ is the calibration factor, which is defined as

$$K_{\mathrm{cal}}(\varphi) = 2\pi f_{\mathrm{RF}} LC_{\mathrm{RFD0a}} \cos(\varphi) = K_{\mathrm{cal}} \cos(\varphi). \tag{10}$$

Sometimes, it can be useful to write the covariance in terms of correlation coefficients (i.e., $\sigma_{ij} = r_{ij}\sigma_i\sigma_j$) to quantify how two quantities are correlated (i.e., $|r_{ij}| = 0$ implies no correlation at all, while if $|r_{ij}| = 1$, the variables i and j are strongly correlated).

Comparing (8) with (10), under the same assumption used in (8), the relationship between the vertical bunch centroid and the calibration factor is [3]

$$K_{\mathrm{cal}} = 2\pi f_{\mathrm{RF}} \frac{dC_{y_s}}{d\varphi}. \tag{11}$$

Measuring the vertical bunch centroid while varying the deflecting voltage phase in a small range around the voltage zero crossing (i.e., $\varphi = 0$ rad and $\varphi = \pi$ rad), the derivative $dC_{y_s}/d\varphi$ can be calculated as the slope p of the bunch centroid versus the RFD phase φ. Therefore, the calibration factor can be directly calculated by measuring the bunch centroid positions at the measurement screen for different values of the deflecting phase, knowing only the deflecting voltage frequency. Namely, the measurements can be self-calibrated [3], without measuring directly C_{RFD0a} from (4). In the typical RF system used in LINACs (dealing with tens of megawatt power), the direct measurement of V_t is affected by poor accuracy (mainly due to directional couplers used in practice), and thus, (4) is never exploited to compute C_{RFD0a}. As pointed out in Section I, such a self-calibration is a key feature of this technique.

III. New Measurement Methods

In this section, two measurement methods for energy chirp and spread (see Section III-A) and correlations between particle positions, divergences, and energies (see Section III-B) are stated.

A. Energy Chirp and Spread

In the following, the theory behind the measurement method is introduced (see Section III-A1). Then, the steps of the model of measurement production are detailed (see Section III-A2) [28].

1) Theory: The fifth and the sixth terms of (9) can be canceled by averaging between $\sigma_{y_s}^2(\varphi)$ and $\sigma_{y_s}^2(\varphi + \pi)$. Furthermore, considering a small range of the deflecting voltage phase around the voltage zero crossing, it is possible to write

$$\begin{aligned} A^2(\varphi_i) &= \frac{\sigma_{y_s}^2(\varphi_i) + \sigma_{y_s}^2(\varphi_i + \pi)}{2} \\ &= \sigma_{y_s,\mathrm{OFF}}^2 + K_{\mathrm{cal}}^2 \left[\sigma_{t_0}^2 - \frac{\sigma_{t_0\delta_0}}{\pi f_{\mathrm{RF}}}\varphi_i + \frac{\sigma_{\delta_0}^2}{(2\pi f_{\mathrm{RF}})^2}\varphi_i^2\right] \\ &= p_3 + p_2\varphi_i + p_1\varphi^2 \end{aligned} \tag{12}$$

for each i-measurement. The third and the fourth terms of (12) are the contributions of the energy chirp and spread to the vertical spot size at the measurement screen with the RFD active. They are sources of deterministic errors in the bunch length measurements [22] and are typically calibrated away with independent measurements of σ_{δ_0} and $\sigma_{t_0\delta_0}$. On the other hand, these contributions can be used to measure the energy chirp and spread from vertical spot size measurements versus the deflecting voltage phase. In particular, (12) is a quadratic

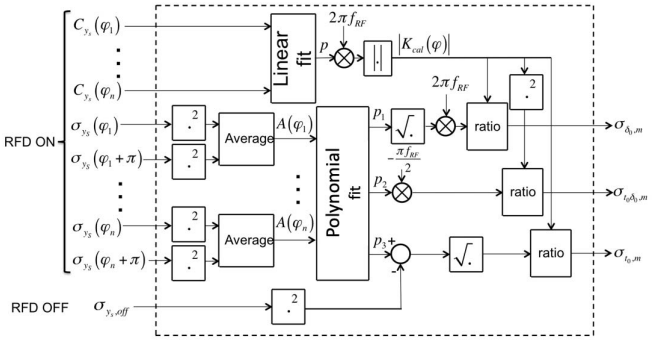

Fig. 2. Model of measurement production for energy spread, energy chirp, and bunch length [28].

polynomial of the variable φ_i. The energy spread, the energy chirp, and the bunch length can be calculated as

$$\sigma_{\delta_0,m} = \sqrt{p_1}\frac{2\pi f_{\mathrm{RF}}}{K_{\mathrm{cal}}} \tag{13}$$

$$\sigma_{t_0\delta_0,m} = -p_2\frac{2\pi f_{\mathrm{RF}}}{2K_{\mathrm{cal}}^2}, \text{ and } \sigma_{t_0,m} = \frac{\sqrt{p_3 - \sigma_{y_s,\mathrm{OFF}}^2}}{K_{\mathrm{cal}}} \tag{14}$$

where p_1, p_2, and p_3 are the coefficients of the polynomial fits defined in (13) and (14). Some further considerations from (12) can be made. First, in the vertical spot size, the first term should be non-dominant with respect to the other terms, because the other terms contain information about the measurands: the bunch length (i.e., $\sigma_{t_0,m}$), energy chirp (i.e., $\sigma_{t_0\delta_0,m}$), and energy spread (i.e., $\sigma_{\delta_0.m}$). With this aim, K_{cal} can be increased (namely, the distance between the RFD and the screen and/or the deflecting voltage amplitude) and $\sigma_{y_s,\mathrm{OFF}}$ can be decreased, by means of vertical focusing quadrupoles placed before the RFD. Moreover, the second, the third, and the fourth term of (12) should have individually a non-negligible impact on vertical spot size. These contributions include the same coefficient K_{cal}^2; therefore, for a fixed deflecting voltage frequency, the variations of the distance between the RFD and the screen, and/or the deflecting voltage amplitude, do not alter the contribution of each term to the vertical spot size. The proposed measurement method can be applied only when the measurands give a non-negligible contribution to the vertical spot size, i.e., for bunch with suitable properties in terms of length, energy chirp, and energy spread. When the energy spread contribution is negligible [fourth terms in (12)], $A^2(\varphi)$ becomes a straight line in function of the deflecting voltage phase (examples given in Section IV).

2) Model of Measurement Production: The previous theory suggests a measurement method based on the RFD not only for the bunch length (standard approach) but also for the energy chirp and spread. The bunch length measurement model, shown in Fig. 2, is first based on the measurements of the spot size at the screen when the RFD is off-line (i.e., obtaining $\sigma_{y_s,\mathrm{OFF}}$). Later, by switching ON the RFD, the vertical bunch centroid and spot size at the screen can be measured for different values of the RFD phase φ_i [i.e., obtaining $C_{y_s}(\varphi_i)$, $\sigma_{y_s}(\varphi_i)$, and $\sigma_{y_s}(\varphi_i+\pi)$]. As a second step (data processing), the calibration factor K_{cal} is computed with (11); thus applying (12), also, the coefficients p_1, p_2, and p_3 are computed by means of a polynomial fit. As a last step, using (13) and (14), the measured energy spread ($\sigma_{\delta_0,m}$), energy chirp ($\sigma_{t_0\delta_0,m}$), and bunch length ($\sigma_{t_0,m}$) are obtained.

The presented model requires new steps of data acquisition and elaboration with respect to the standard method of the bunch length measurement [22]. First, different vertical spot size measurements are needed, in order to cancel the contributions due to the correlations among positions, divergences, and energies at the RFD entrance. Second, a polynomial fit of the squared values of the vertical spot size at the screen varying the RFD phase is required.

B. Correlations Between Particle Positions, Divergences, and Energies

In this section, the measurement method for the correlations between particle positions, divergences, and energies is exposed [29]. First, the underlying theory is explained (Section III-B1). Later, the model of measurement production is described (Section III-B2).

1) Theory: As reported in [12], the contributions given by the correlations between particle positions, divergences, and energies at RFD entrance [through an average between $\sigma_{y_s}^2(\varphi)$ and $\sigma_{y_s}^2(\varphi+\pi)$ as shown in (12)] can be corrected. On the other hand, the variations of the squared value of vertical spot size due to these correlations can be used to measure them. The idea relies on the following property; for the deflecting voltage phases φ and $\varphi+\pi$, all the terms of $\sigma_{y_s}^2$ (9) do not change their signs and values, but the correlation contributions change their sign. Therefore, the correlation terms can be isolated by taking the differences of the squared values of the vertical spot size at the screen around the two zero-crossing phases (using the approximation of a small phase φ around 0 rad)

$$\begin{aligned}\mathrm{cor}_{l_0v_0}(\varphi) &= \frac{\sigma_{y_s}^2(\varphi) - \sigma_{y_s}^2(\varphi+\pi)}{2} \\ &= 2K_{\mathrm{cal}}\mathrm{cor}_{t_0v_0} - 2\frac{K_{\mathrm{cal}}}{2\pi f_{\mathrm{RF}}}\mathrm{cor}_{\delta_0v_0}\varphi \\ &= q_{\mathrm{cor}} + p_{\mathrm{cor}}\varphi\end{aligned} \tag{15}$$

where

$$\mathrm{cor}_{t_0v_0} = \sigma_{y_0t_0} + L\sigma_{y_0't_0} \text{ and } \mathrm{cor}_{\delta_0v_0} = \sigma_{y_0\delta_0} + L\sigma_{y_0'\delta_0}. \tag{16}$$

The information about the correlations can be found with a linear fit of $\mathrm{cor}_{l_0v_0}(\varphi)$; thus, the measured values are

$$\mathrm{cor}_{\delta_0v_0,m} = -\frac{\pi f_{\mathrm{RF}}}{K_{\mathrm{cal}}}p_{\mathrm{cor}} \text{ and } \mathrm{cor}_{t_0v_0,m} = \frac{q_{\mathrm{cor}}}{2K_{\mathrm{cal}}}. \tag{17}$$

2) Model of Measurement Production: The model of measurement production for the correlation terms is shown in Fig. 3. The model relies on measurement and data processing. The first stage consists of the measurements of the vertical bunch centroid position and spot size at the screen for different values of the deflecting voltage phase φ_i (close to the zero crossing), obtaining $C_{y_s}(\varphi_i)$, $\sigma_{y_s}(\varphi_i)$, and $\sigma_{y_s}(\varphi_i+\pi)$. Afterward, one can compute the calibration factor K_{cal} from (11), the coefficients p_{cor} and q_{cor} as well as evaluate the correlation terms $\mathrm{cor}_{\delta_0v_0,m}$ and $\mathrm{cor}_{t_0v_0,m}$ from (17).

TABLE I
VIRTUAL MEASUREMENT PARAMETERS AND RESULTS

Case study	σ_{t_0} [fs]	$\sigma_{t_0,m}$ [fs]	$E_{\sigma_{t_0,m}}$	σ_{δ_0} [%]	$\sigma_{\delta_0,m}$ [%]	$E_{\sigma_{\delta_0,m}}$	$\sigma_{t_0\delta_0}$[fs]	$\sigma_{t_0\delta_0,m}$[fs]	$E_{\sigma_{t_0\delta_0,m}}$
Compton inj.	912	907.9 (3.0)	0.4%	0.6054	...	....	5.329	5.06 (38)	5.0%
FEL inj. I	250	250.86 (23)	0.3%	1	0.8932 (99)	10.7%	-2.06	-2.070 (34)	0.5%
FEL inj. II	25	24.84 (10)	0.6%	0.5	0.4973 (10)	0.5%	0.1125	0.10870 (36)	3.4%
Plasma acc. I	100	100.21 (22)	0.2%	1	0.9824 (42)	1.8%	0.965	0.9542 (25)	1.2%
Plasma acc. II	10	9.70860 (97)	2.9%	4	4.0094 (32)	0.2%	0.36	0.3400 (48)	5.5%

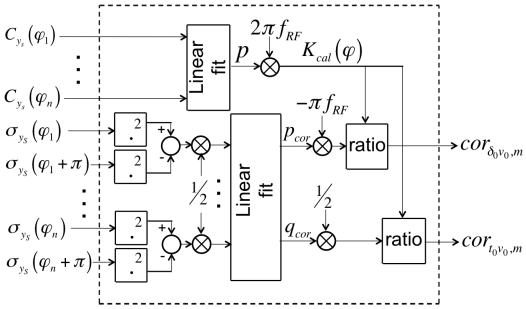

Fig. 3. Model of measurement production for correlation terms between the longitudinal and vertical planes [29].

IV. NUMERICAL RESULTS

The case studies concern different kinds of high-brightness electron LINACs for radiation sources, very relevant in the worldwide research and development effort on novel particle accelerators. Some peculiar examples of Compton sources in Section IV-A, FEL injectors in Section IV-B, and plasma based accelerators in Section IV-C are discussed. These three machines use electron bunches with different values of σ_{t_0}, σ_{δ_0}, and $\sigma_{t_0\delta_0}$. In Section IV-D, the proposed measurement model production of the correlation terms is applied to a case study. The Compton source case study is the GBS LINAC, and the parameters used in the numerical studies are obtained from the start-to-end simulations used in the design of the machine [18]. For the other two cases (i.e., FELs and plasma accelerators), two different sets of bunch properties meaningful for a large number of machines are presented.

The bunch longitudinal parameters (i.e., σ_{t_0}, σ_{δ_0}, and $\sigma_{t_0\delta_0}$) are reported in Table I as well as the foreseen measurement results (i.e., $\sigma_{t_0,m}$, $\sigma_{\delta_0,m}$, and $\sigma_{t_0\delta_0,m}$). For reader convenience, a column with the relative percentage deterministic error for each quantity X with measured value X_m has been added (i.e., $E_{X_m} = 100 \cdot |X - X_m|/X$); the values have been truncated to improve readability.

The RFD deflector parameters used in the simulations ($V_t = 1$ MV and $f_{\mathrm{RF}} = 2.856$ GHz) are extremely conventional and they can be achieved by most of the high-brightness LINACs nowadays in operation. The distance of the measurement screen from the RFD is $L = 1.138$ m, and the beam energy is $\langle E_0 \rangle = 118$ MeV; those values are the ones used in GBS and they have been kept constant also in the other examples because they are quite common and reasonable.

It is worth noting that the variation of the rms vertical spot size needed in all the case studies is in the order of few tens of micrometers and it may require advanced diagnostic tools. The beam vertical dimension on the measurement screen can be increased: 1) in percentage, using a better magnetic optics when the RFD is switched OFF (to decrease $\sigma_{y_{s,\mathrm{OFF}}}$) and 2) in absolute terms, increasing the deflecting voltage amplitude and/or the distance between the RFD and the measurement screen (to increase K_{cal}).

A bunch composed of 50,000 macroparticles (with a total charge of 250 pC for the GBS case, 100 pC in the FEL cases, and 10 pC for the plasma cases) was tracked by ELEGANT through the RFD up to the measurement screen. The bunch is traveling on axis ($C_{y_0} = 0$ m and $C_{y'_0} = 0$ rad).

The use of state-of-the-art tracking codes as metrological reference is a standard procedure in particle accelerator design and engineering, both in a single system (as done in this article) and as the particle accelerator layout as a whole. ELEGANT code is well established and it has been, through years, validated against a huge number of different practical cases; nowadays, it is exploited in the LINACs design as well as commissioning. Moreover, ELEGANT simulations are considered so reliable that are also used to detect measurement artifacts, especially in the accelerator commissioning or development. Such approach is mandatory in complex particle accelerator systems where particularly challenging beam conditions can be accessed only when the accelerator is built (e.g., GBS).

A. Compton Sources—Gamma Beam Source

In the GBS injector, a 250 pC beam of a nominal bunch length of 1 ps with few ‰ energy spread is delivered to the interaction chamber (a laser beam circulator [30]) to collide with the laser photons. In the case study, the used beam parameter values (first row of Table I) are results of start-to-end simulations of the whole LINAC before the RFD, according to [18] and, therefore, they are representative of a real beam. Fig. 4 shows the longitudinal phase space, while the bunch length, energy chirp, and energy spread are given in Table I.

In this case study, the energy chirp contribution to the vertical spot size is significant, while the energy spread contribution is negligible. Thus, only the energy chirp can be measured by means of the proposed measurement method, i.e., through a linear fit of the vertical spot size versus the deflecting voltage phase, as shown in Table I.

The vertical bunch centroid and spot size measurements, while varying the deflecting voltage phase, are shown in Fig. 5(a) and (b), respectively. The centroid variation with respect to the RFD phase can be used to compute K_{cal} from (11). The uncertainty on K_{cal} as well as the measured energy chirp and bunch length is only due to the linear fit.

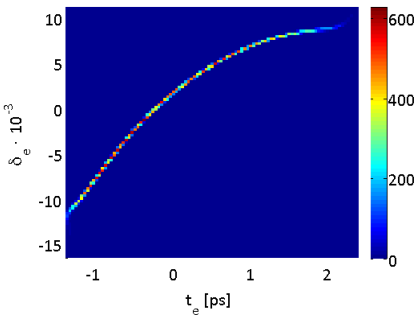

Fig. 4. Longitudinal trace space at RFD entrance ($\sigma_{t_0} = 0.9118$ ps, $\sigma_{\delta_0} = 6.054 \cdot 10^{-3}$, and $\sigma_{t_0\delta_0} = 5.329$ fs). The beam transverse parameters at the RFD entrance are: $\sigma_{y_0} = 346.4$ μm, $\sigma_{y_0'} = 57.57$ μrad, and $\sigma_{y_0 y_0'} = -19.86$ nm. All those values are obtained by start-to-end simulations for the GBS machine.

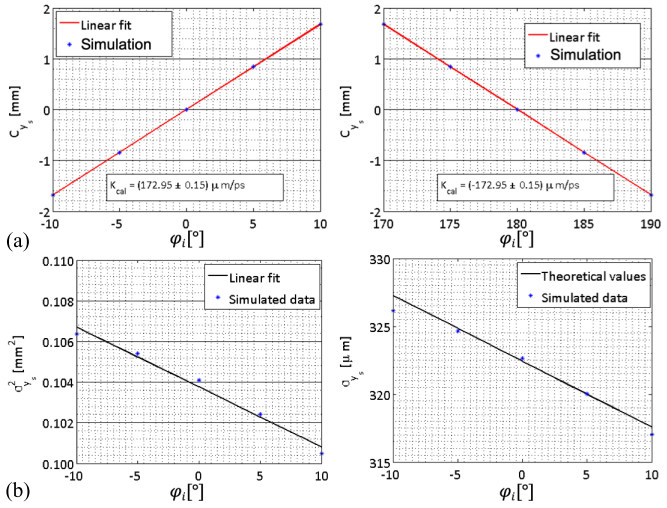

Fig. 5. (a) Vertical bunch centroids and (b) spot sizes at the screen versus φ_i. Simulated data reported as stars and linear fit as solid line. The centroids are taken around the two RFD voltage zero crossings (φ_i around 0 and π); from the linear fit, one could measure the calibration constant, getting $|K_{\text{cal}}| = (172.95 \pm 0.15)$ μm/ps. The second line shows σ_{y_s} and $\sigma^2_{y_s}$ around the first RFD voltage zero crossing (φ_i between $-10°$ and $10°$). The rms spot size when the RFD is switched OFF is $\sigma_{y_{s,\text{OFF}}} = 281$ μm.

The approximation of a constant calibration factor in the RFD phase range leads to a relative error less than 1.5% and thus negligible with respect to the theoretical calibration factor (10).

Since the energy spread contribution is negligible, the squared value of the vertical spot size is linear (12) over the deflecting voltage phase range [see the left of Fig. 5(b)]. The averages of the squared values of vertical spot size at the screen are not affected by significant inaccuracy because the correlations between the vertical and longitudinal planes are weak [see the right of Fig. 5(b)].

B. Free Electron Laser Sources

The second case study concerns two extreme cases of LINAC used as injector for FELs. Case I is a 250 fs long bunch with a moderate energy spread and a strong energy chirp (correlation factor $r_{t_0\delta_0} = -0.8$). Similar, i.e., energy-chirped, high-brightness electron beams have been used for single-spike

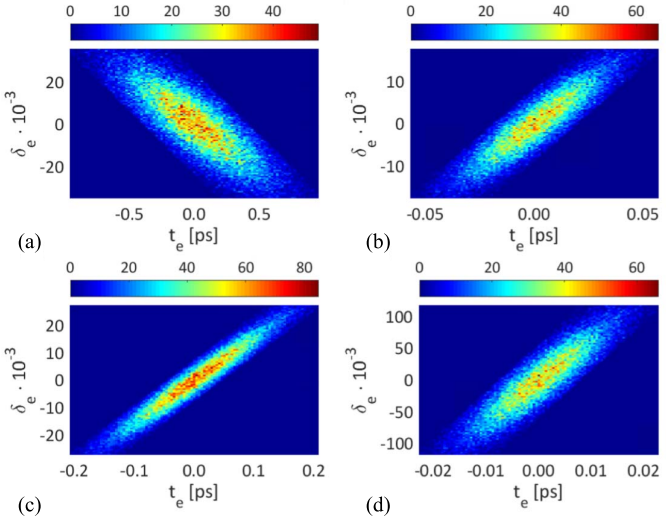

Fig. 6. Longitudinal trace space at RFD entrance. The first row concerns the FEL injector (a) case I and (b) case II. The second row concerns plasma accelerator (c) case I and (d) case II. The beam longitudinal beam parameters are given in Table I.

FEL radiation [31], [32]. The longitudinal phase space at the RFD entrance is given in Fig. 6(a), where the negative value of the energy chirp is clear. Case II deals with novel ideas being discussed in the scientific community on future FEL injectors, aiming to a much higher beam current (in the few kiloampere range) than conventional FELs. If those currents are reached while keeping a small energy spread (e.g., half of the one considered in case I), ultrahigh brightness can be reached. This implies a strong reduction in the length using undulator magnets, which are nowadays limiting the compactness of FELs. A positive strong chirps, with a high correlation factor $r_{t_0\delta_0} = 0.9$, is considered [longitudinal phase space at the RFD entrance is given in Fig. 6(b)]. The spot size variation at the measurement screen when the RFD is switched ON is quite relevant (50% for case I). In Table I, the second and third rows report the estimations of the longitudinal parameters and the relative errors. In the second example, the error of the measured energy spread is larger than the first case, because the contribution of the bunch length term to the vertical spot size is larger, but the contribution of the energy spread term does not increase (9).

C. Plasma Based Particle Accelerators

Plasma based particle accelerators are undergoing an intense development. The huge accelerating fields (three orders of magnitude larger than conventional RF field used in accelerators) require a high degree of control of the beam parameters to reach the same stability and reliability of conventional accelerators. At the moment, several solutions are being investigated [33], ranging from laser- to particle-driven accelerators. The two case studies reported in this section are representative of two typical cases. Case I concerns with about 100 fs beam and 1% energy spread, compatible with particle driven solutions, whereas Case II investigates ultrashort bunches (10 fs), with big energy spreads (4%) similar to laser-driven experiments. Both the cases exhibit quite strong

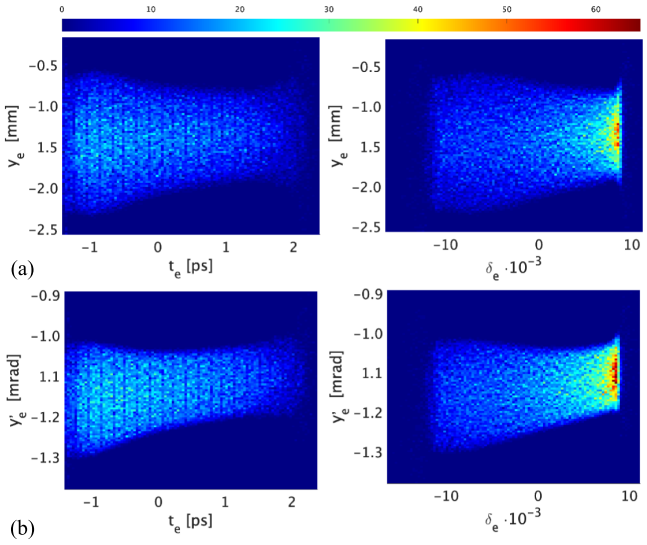

Fig. 7. (a) Particle vertical positions versus longitudinal positions with $r_{y_0t_0} = 0.12$ (left) and particle energies with $r_{y_0\delta_0} = 0.11$ (right). (b) Particle vertical divergences versus longitudinal positions with $r_{y'_0t_0} = 0.29$ (left) and particle energies with $r_{y'_0\delta_0} = 0.28$ (right). All the data are virtually measured at the RFD entrance, being $\sigma_{y_0} = 348.8$ μm, $\sigma_{y'_0} = 60.15$ μrad, and $\sigma_{y_0y'_0} = -19.15$ nm.

energy chirps (correlation coefficient almost 1), a so typical situation in plasma accelerator that specific solutions are being addressed [34]. Longitudinal phase spaces of the beam at the RFD entrance are shown in Fig. 6(c) and (d) for cases I and II, respectively. Table I reports the specific numerical values. Applying the proposed technique, the percentage variation of the rms vertical spot size at the screen is again about 50% when the RFD is switched ON. Table I reports the expected measured values, as well as the relative measurement error.

D. Measurements of the Correlation Among Particle Positions, Divergences, and Energies

As abovementioned, the proposed measurement method can be applied only if the correlation terms give a not negligible contribution to the vertical spot size measurements [see (9)]. Therefore, this points out a threshold for carrying out the measurement method with acceptable accuracy. The contribution of the correlation terms on the vertical spot size at the measurement screen can become negligible in the case of longer bunches. In this respect, the analysis is restricted to the most challenging case study with the longest bunches, namely the GBS. In the following, the simulation conditions (Section IV-D1) and the measurements of the correlation terms (Section IV-D2) are illustrated.

1) Simulation Conditions: The correlations between particle positions, divergences, and energies are unwanted effects, possibly caused by misalignments, position jitters, field imperfections, and so on. The considered correlations could be caused by a 2 mm misalignment of the first accelerating section and the focusing (quadrupole) magnet upstream of the RFD; such a misalignment is within the design tolerance of the machine. Fig. 7 reports the relevant trace spaces obtained by a start-to-end simulation of the whole machine

TABLE II

VIRTUAL MEASUREMENT AND DATA PROCESSING RESULTS FROM (11) AND (17)

	Reference value	Measured value	Relative error
K_{cal} $\varphi \approx 0$ rad	173.7 μm/ps	172.81 (15) μm/ps	≈ 0.5%
K_{cal} $\varphi \approx \pi$ rad	−173.7 μm/ps	−173.10 (15) μm/ps	≈ 0.1%
$cor_{t_0v_0}$	54.96 μm ps	54.35 (21) μm ps	≈ 1%
$cor_{\delta_0v_0}$	0.3499 μm	0.348 (29) μm	≈ 0.5%

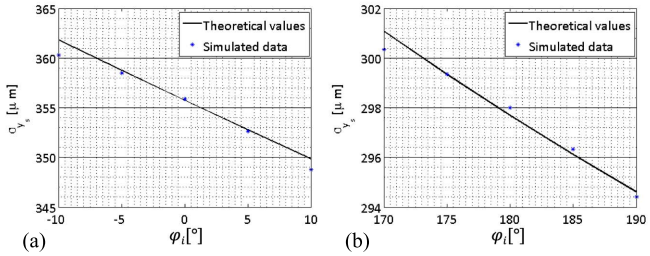

Fig. 8. Vertical spot size at the screen over the deflecting voltage range of (a) −10° to 10° and (b) 170°–190°. Simulated data in blue stars and theoretical values (9) in solid line.

(i.e., upstream the RFD) considering the misalignments; the proposed measurement technique aims to estimate the correlations by measuring spot sizes of RFD deflected beam at the measurement screen.

2) Measurements of the Correlation Terms: Applying the model of the measurement production to the case study, the virtual measurement and the data processing results are reported in Table II. The approximation of a constant calibration factor (calculated from vertical centroid measurements) in the RFD phase range leads to a negligible relative error compared with the theoretical calibration factor. The uncertainty on the correlations terms is only due to the linear fits.

The vertical bunch centroid measured while varying the deflecting voltage phase shows the same slope of the case without misalignment. The differences between Fig. 8(a) and (b) are caused by the significant correlation contributions to the vertical spot size at the screen.

From these results and Fig. 5, the requirements on the resolution of the optical system using to image the beam footprint on an acquisition camera can be assessed and compared with the optical issues for the diagnostic stations [35], [36]. Weaker correlations imply smaller correlation terms (i.e., small variations of the vertical spot size at the screen) and, therefore, they require better resolution.

V. CONCLUSION

In this article, a method for measuring the longitudinal bunch parameters, as well as the correlations between particle positions, divergences, and energies, is proposed. The theory of the RFD-based measurement was extended to quantify the effect of energy chirp and correlation terms, by opening the way to define two models of measurement production of

those quantities. The possibility of measuring energy spread and chirps by means of only the RFD is particularly interesting for novel high-brightness LINACs. To assess the validity and accuracy of the method, the result of a virtual measurement campaign carried out by a tracking code used in the design and commissioning of modern particle accelerators (ELEGANT) is reported. The case studies covered all the kinds of LINACs being designed or operated as radiation sources (i.e., Compton sources and FELs), as well as LINACs designed to exploit the plasma acceleration. In all those cases, the relative error of the measured energy chirp, obtained using the proposed technique, is around 5%. In the case of GBS, when strong correlations due to machine misalignment may be present, relative errors of the correlation term measurements are below 1%.

ACKNOWLEDGMENT

The research activity was carried out at the Istituto Nazionale di Fisica Nucleare-Laboratori Nazionali di Frascati (INFN-LNF) under the framework of the European project extreme light infrastructure to study nuclear physics (ELI-NP). The authors would like to thank David Alesini, Enrica Chiadroni, Alessandro Cianchi, Anna Giribono, Annalisa Liccardo, Valerio Pettinacci, and Cristina Vaccarezza for their useful discussion and suggestions.

REFERENCES

[1] X. J. Wang, "Producing and measuring small electron bunches," in *Proc. Part. Accel. Conf.*, New York, NY, USA, 1999, pp. 229–233.
[2] G. A. Loew *et al.*, "Design and application of RF separator structures at SLAC," in *Proc. 5th Int. Conf. High-Energy Accel.*, Frascati, Italy, 1965, pp. 438–442.
[3] D. Alesini *et al.*, "Sliced beam parameter measurements," in *Proc. DIPAC*, Basel, Switzerland, 2009, pp. 1–5.
[4] A. Cianchi, "Observations and diagnostics in high brightness beams," in *Proc. CERN Accel. School (CAS), Intensity Limitations Particle Beams*, Geneva, Switzerland, Nov. 2015, pp. 343–347.
[5] D. Alesini *et al.*, "RF deflector design and measurements for the longitudinal and transverse phase space characterization at SPARC," *Nucl. Instrum. Methods Phys. Res. A, Accel. Spectrom. Detect. Assoc. Equip.*, vol. 568, no. 2, pp. 488–502, Dec. 2006.
[6] C. Vaccarezza *et al.*, "The SPARC Lab Thomson source," *Nucl. Instrum. Methods Phys. Res. A, Accel. Spectrom. Detect. Assoc. Equip.*, vol. 829, pp. 237–242, Oct. 2016.
[7] R. Pompili *et al.*, "Beam manipulation with velocity bunching for PWFA applications," *Nucl. Instrum. Methods Phys. Res. A, Accel. Spectrom. Detect. Assoc. Equip.*, vol. 829, pp. 17–23, Sep. 2016.
[8] L. Sabato *et al.*, "Metrological characterization of the bunch length system measurement of the ELI-NP electron LINAC," in *Proc. 14th IMEKO TC10*, Milan, Italy, 2016, pp. 203–208.
[9] S. M. Shajedul Hasan, Y. W. Kang, and M. K. Howlader, "Development of an RF conditioning system for charged-particle accelerators," *IEEE Trans. Instrum. Meas.*, vol. 57, no. 4, pp. 743–750, Apr. 2008.
[10] P. Arpaia, R. Corsini, A. Gilardi, A. Mostacci, L. Sabato, and K. N. Sjobak, "Enhancing particle bunch-length measurements based on radio frequency deflector by the use of focusing elements," *Sci. Rep.*, vol. 10, no. 1, pp. 1–12, 2020.
[11] S. Tang, L. Zhao, S. Liu, X. Hao, W. Wu, and Q. An, "A beam phase and energy measurement instrument based on direct RF signal IQ undersampling technique," *IEEE Trans. Instrum. Meas.*, vol. 61, no. 11, pp. 2870–2878, Nov. 2012.
[12] L. Sabato *et al.*, "Effects of correlations between particle longitudinal positions and transverse plane on bunch length measurement: A case study on GBS electron LINAC at ELI-NP," *Meas. Sci. Technol.*, vol. 29, no. 2, Feb. 2018, Art. no. 024005.
[13] A. Mostacci *et al.*, "Chromatic effects in quadrupole scan emittance measurements," *Phys. Rev. Special Topics-Accel. Beams*, vol. 15, no. 8, Aug. 2012, Art. no. 082802.
[14] A. Cianchi *et al.*, "Six-dimensional measurements of trains of high brightness electron bunches," *Phys. Rev. Special Topics-Accel. Beams*, vol. 18, no. 8, Aug. 2015, Art. no. 082804.
[15] A. Cianchi *et al.*, "Challenges in plasma and laser wakefield accelerated beams diagnostic," *Nucl. Instrum. Methods Phys. Res. A, Accel. Spectrom. Detect. Assoc. Equip.*, vol. 720, pp. 153–156, Aug. 2013.
[16] A. Garzon-Camacho, B. Fernandez, M. A. G. Alvarez, J. Ceballos, and J. M. de la Rosa, "A fast readout electronic system for accurate spatial detection in ion beam tracking for the next generation of particle accelerators," *IEEE Trans. Instrum. Meas.*, vol. 64, no. 2, pp. 318–327, Feb. 2015.
[17] J. Gao, "Effects of the cavity walls on perturbation measurements," *IEEE Trans. Instrum. Meas.*, vol. 40, no. 3, pp. 618–622, Jun. 1991.
[18] O. Adriani *et al.*, "Technical design report EuroGammaS proposal for the ELI-NP gamma beam system," 2014, *arXiv:1407.3669*. [Online]. Available: http://arxiv.org/abs/1407.3669
[19] C. A. Ur *et al.*, "The ELI–NP facility for nuclear physics," *Nucl. Instrum. Methods Phys. Res. B, Beam Interact. Mater. At.*, vol. 355, pp. 198–202, Jul. 2015.
[20] M. Ferrario *et al.*, "EuPRAXIA@ SPARC_LAB design study towards a compact FEL facility at LNF," *Nucl. Instrum. Methods Phys. Res. A, Accel. Spectrom. Detect. Assoc. Equip.*, vol. 909, pp. 134–138, Nov. 2018.
[21] M. Borland, "Elegant: A flexible SDDS-compliant code for accelerator simulation," Argonne Nat. Lab., Lemont, IL, USA, Tech. Rep. LS-287, 2000.
[22] L. Sabato *et al.*, "Effects of energy chirp on bunch length measurement in linear accelerator beams," *Meas. Sci. Technol.*, vol. 28, no. 8, Aug. 2017, Art. no. 084002.
[23] K. Floettmann and V. V. Paramonov, "Beam dynamics in transverse deflecting RF structures," *Phys. Rev. Special Topics-Accel. Beams*, vol. 17, no. 2, Feb. 2014, Art. no. 024001.
[24] R. Akre, L. Bentson, P. Emma, and P. Krejcik, "A transverse RF deflecting structure for bunch length and phase space diagnostics," in *Proc. Part. Accel. Conf. (PACS)*, 2001, pp. 2353–2355.
[25] L. Sabato, "Bunch length measurements in the gamma beam system linac by means of an RF deflector at ELI–NP," Ph.D. dissertation, Univ. Sannio, Benevento, Italy, 2017.
[26] L. Sabato *et al.*, "Metrological characterization of the bunch length measurement by means of a RF deflector at the ELI- -NP Compton gamma source," in *Proc. Int. Part. Accel. Conf. (IPAC)*, Busan, South Korea. Geneva, Switzerland: JACoW, May 2016, pp. 122–125, Paper MOPMB018.
[27] H. Wiedemann, *Particle Accelerator Physics*. Springer, 2015.
[28] L. Sabato, P. Arpaia, A. Liccardo, A. Mostacci, L. Palumbo, and A. Variola, "Energy chirp measurements by means of an RF deflector: A case study the gamma beam source LINAC at ELI–NP," in *Proc. Int. Part. Accel. Conf. (IPAC)*, Copenhagen, Denmark. Geneva, Switzerland: JACoW, May 2017, pp. 242–245, Paper MOPAB059.
[29] L. Sabato, P. Arpaia, A. Liccardo, A. Mostacci, L. Palumbo, and A. Variola, "RF deflector based measurements of the correlations between vertical and longitudinal planes at ELI–NP–GBS electron LINAC," in *Proc. Int. Beam Instrum. Conf. (IBIC)*, Grand Rapids, MI, USA, Aug. 2017, pp. 1–4, Paper WEPCC20.
[30] C. F. Ndiaye *et al.*, "Low power commissioning of an innovative laser beam circulator for inverse Compton scattering γ-ray source," *Phys. Rev. A, Gen. Phys.*, vol. 22, no. 9, Sep. 2019, Art. no. 093501, doi: 10.1103/PhysRevAccelBeams.22.093501.
[31] L. Giannessi *et al.*, "Self-amplified spontaneous emission free-electron laser with an energy-chirped electron beam and undulator tapering," *Phys. Rev. Lett.*, vol. 106, no. 14, 2011, Art. no. 144801.
[32] G. Marcus *et al.*, "Time-domain measurement of a self-amplified spontaneous emission free-electron laser with an energy-chirped electron beam and undulator tapering," *Appl. Phys. Lett.*, vol. 101, no. 13, Sep. 2012, Art. no. 134102.
[33] M. K. Weikum *et al.*, "EuPRAXIA—A compact, cost-efficient particle and radiation source," in *Proc. 25th Int. Conf. Appl. Accel. Res. Ind.*, vol. 2160, 2019, Art. no. 040012.
[34] V. Shpakov *et al.*, "Longitudinal phase-space manipulation with beam-driven plasma wakefields," *Phys. Rev. Lett.*, vol. 122, no. 11, Mar. 2019, Art. no. 114801.
[35] M. Marongiu *et al.*, "Optical issues for the diagnostic stations for the ELI–NP Compton gamma source," in *Proc. Int. Part. Accel. Conf. (IPAC)*, Copenhagen, Denmark. Geneva, Switzerland: JACoW, May 2017, pp. 238–241, Paper MOPAB058.
[36] F. Cioeta *et al.*, "Spot size measurements in the ELI–NP Compton gamma source," in *Proc. Int. Beam Instrum. Conf. (IBIC)*, Barcelona, Spain. Geneva, Switzerland: JACoW, Sep. 2016, pp. 532–535, Paper TUPG74.

Luca Sabato was born in Busto Arsizio, Italy, in 1987. He received the M.Sc. degree (Hons.) in telecommunication engineering, the M.S. degree (Hons.) in electronic engineering, and the Ph.D. degree in information technology for engineering from the University of Sannio, Benevento, Italy, in 2010, 2013, and 2017, respectively. His Ph.D. research on beam diagnostics, in particular bunch length measurements in LINACs by means of radio frequency deflectors, was carried out at the Istituto Nazionale di Fisisca Nucleare–Laboratori Nazionali di Frascati (INFN-LNF), Frascati, Italy.

From June 2013 to December 2013, he was with the Sources, Targets and Interactions Group, Engineering Department, European Organization for Nuclear Research (CERN), Geneva, Switzerland, where he worked on modeling parasitic capacitances effects on ironless inductive position sensors. Since January 2018, he has been working as a Senior Fellow at the Beam Department, CERN, carrying out research activity on beam instabilities driven by electron cloud in the Large Hadron Collider (LHC). His main research interests are studies on electron cloud effects in particle accelerators, measurement techniques, and instrumentation for particle accelerators.

Pasquale Arpaia (Senior Member, IEEE) received the master's degree and the Ph.D. degree in electrical engineering from the University of Naples Federico II, Naples, Italy, in 1987 and 1992, respectively.

He is currently a Full Professor of instrumentation and measurements with the University of Naples Federico II. He was a Professor with the University of Sannio, Benevento, Italy, an Associate Professor with the Institutes of Engines and Biomedical Engineering, CNR, Rome, Italy, and the INFN Section, Naples. He is also the Head of different research groups, IMPALab, ARHeMlab, and FabLab. He is also the Deputy Chairman of CIRMIS and the Chairman of the Stage Project at the University of Naples Federico II. He was the scientific responsible of more than 30 awarded research projects in cooperation with industry, with related patents and international licenses, and funded four academic spin-off companies. He acted as a scientific evaluator in several international research call panels. His main research interests include instrumentation and measurement for many sectors in the accelerator technology field and several different biomedical fields. In these fields, he has published three books, several book chapters, and about 300 scientific papers in journals and national and international conference proceedings.

Dr. Arpaia continuously serves as organizing and scientific committee member in IEEE and IMEKO conferences. He is a plenary speaker at several scientific conferences.

Antonio Gilardi (Graduate Student Member, IEEE) received the M.S. degree *(cum laude)* in electronic engineering from the University of Naples Federico II, Naples, Italy, in 2017. He is currently pursuing the Ph.D. degree in electronics with the Department of Electrical Engineering and Information Technology, University of Naples Federico II, in collaboration with the European Organization for Nuclear Research (CERN), Geneva, Switzerland.

He has been part of the IMPALab Laboratory since 2016. He was with the Hadron Synchrotron Collective effects in the Beam Department, CERN, where he worked on modeling new devices to damp parasitic resonances. He is currently a part of the operation team of the CERN Accelerator for Research (CLEAR), in which he is responsible for different research lines. His current research interests include advance beam diagnostic in particular related to the measurements of the bunch length monitoring system in a particle accelerator and direct measurement of wakefield in new technology X-band accelerating structure.

Andrea Mostacci graduated in electronic engineering at the Sapienza University of Rome, Rome, Italy, in 1997. He received the Ph.D. degree in applied electromagnetism and electro-physical science from the Sapienza University of Rome in 2001.

He started his career in the field of engineering of particle accelerators at CERN, Geneva, Switzerland, the Sapienza University of Rome, and the Laboratori Nazionali di Frascati (Frascati), Istituto Nazionale di Fisica Nucleare (INFN), Frascati, Italy. He is currently an Associate Professor in physics with the Sapienza University of Rome, where he teaches microwave measurements. He has authored or coauthored over 230 publications. His main fields of activity include beam–wall interaction in particle accelerators, coupling impedance and wakefields, design and measurements for RF devices for beam diagnostics and manipulation, high brightness photoinjectors for free electron lasers and radiation sources, laser–plasma interaction for particle acceleration, terahertz sources, gamma rays Compton sources, as well as medical and industrial application of particle accelerators.

Luigi Palumbo graduated in electronic engineering from the University of Naples Federico II, Naples, Italy, in 1979.

He started his career in the field of applied electromagnetism and particle accelerators at KFA, Jülich, Germany, CERN, Geneva, Switzerland, and Laboratori Nazionali di Frascati (Frascati), Istituto Nazionale di Fisica Nucleare (INFN), Frascati, Italy. He is currently a Full Professor in physics with the Sapienza University of Rome, Rome, Italy. He has authored or coauthored over 260 publications. He has been responsible for several projects concerning particle accelerators for basic science and for application to medicine and industry. His main fields of activity include scattering of electromagnetic waves, beam–wall interaction in particle accelerators, coupling impedance and wakefields, RF and microwave devices for beam diagnostics and manipulation, space charge effects, single-bunch and multibunch instabilities, instability controls via active systems (feedbacks) and via Landau Camping, high-frequency RF devices design, high brightness photoinjectors for free electron lasers, and laser–plasma interaction for proton sources.

Alessandro Variola graduated in physics from the University of Trieste, Trieste, Italy, in 1993. He received the Ph.D. degree in experimental physics from Université Paris-Sud, Orsay, France, in 1998.

He is currently a Research Director with the National Institute for Nuclear Physics (INFN), Frascati, Italy. He was responsible for the Accelerators Department, Laboratoire de l'accélérateur linéaire, Orsay. He managed several projects to design and build large-scale particle accelerators. He has authored or coauthored over 170 publications in the field of physics and application of particle accelerators. His research interests include muon generation and cooling, particle accelerator-based radiation sources, high-power RF couplers, positron sources for novel particle accelerators, optical diagnostics for particle beams, and linear particle accelerators.

Dr. Variola received the CNRS Crystal Medal in 2011.